Title

Characterization and evolution of an activator-independent methanol dehydrogenase from Cupriavidus necator N-1.

Journal

Applied microbiology and biotechnology, 100(11)

ISSN

0175-7598

Authors

Wu, Tung-Yun
Chen, Chang-Ting
Liu, Jessica Tse-Jin
et al.

Publication Date

2016-06-01

DOI

10.1007/s00253-016-7320-3

Peer reviewed

Appl Microbiol Biotechnol (2016) 100:4969–4983
DOI 10.1007/s00253-016-7320-3

Characterization and evolution of an activator-independent methanol dehydrogenase from *Cupriavidus necator* N-1

Tung-Yun Wu[1] · Chang-Ting Chen[1] · Jessica Tse-Jin Liu[1] · Igor W. Bogorad[1] · Robert Damoiseaux[2] · James C. Liao[1]

Received: 2 October 2015 / Revised: 15 December 2015 / Accepted: 13 January 2016 / Published online: 5 February 2016

Abstract Methanol utilization by methylotrophic or non-methylotrophic organisms is the first step toward methanol bioconversion to higher carbon-chain chemicals. Methanol oxidation using NAD-dependent methanol dehydrogenase (Mdh) is of particular interest because it uses NAD^+ as the electron carrier. To our knowledge, only a limited number of NAD-dependent Mdhs have been reported. The most studied is the *Bacillus methanolicus* Mdh, which exhibits low enzyme specificity to methanol and is dependent on an endogenous activator protein (ACT). In this work, we characterized and engineered a group III NAD-dependent alcohol dehydrogenase (Mdh2) from *Cupriavidus necator* N-1 (previously designated as *Ralstonia eutropha*). This enzyme is the first NAD-dependent Mdh characterized from a Gram-negative, mesophilic, non-methylotrophic organism with a significant activity towards methanol. Interestingly, unlike previously reported Mdhs, Mdh2 does not require activation by known activators such as *B. methanolicus* ACT and *Escherichia coli* Nudix hydrolase NudF, or putative native *C. necator* activators in the Nudix family under mesophilic conditions. This enzyme exhibited higher or comparable activity and affinity toward methanol relative to the *B. methanolicus* Mdh with or without ACT in a wide range of temperatures. Furthermore, using directed molecular evolution, we engineered a variant (CT4-1) of Mdh2 that showed a 6-fold higher K_{cat}/K_m for methanol and 10-fold lower K_{cat}/K_m for *n*-butanol. Thus, CT4-1 represents an NAD-dependent Mdh with much improved catalytic efficiency and specificity toward methanol compared with the existing NAD-dependent Mdhs with or without ACT activation.

Keywords Methanol dehydrogenase · Methanol utilization · Directed molecular evolution · High throughput screening

Tung-Yun Wu and Chang-Ting Chen contributed equally to this work.

Electronic supplementary material The online version of this article (doi:10.1007/s00253-016-7320-3) contains supplementary material, which is available to authorized users.

✉ James C. Liao
liaoj@ucla.edu

[1] Department of Chemical and Biomolecular Engineering, University of California, Los Angeles, 420 Westwood Plaza, Los Angeles, CA 90095, USA

[2] Department of Molecular and Medicinal Pharmacology, University of California, Los Angeles, 420 Westwood Plaza, Los Angeles, CA 90095, USA

Introduction

Methanol may become an attractive substrate for bioconversion to chemical commodities due to the abundance of methane. Methanol bioconversions to amino acids using methylotrophic bacteria such as *Methylobacterium* sp. for L-serine (Hagishita et al. 1996) and *Methylobacillus glycogenes* for L-threonine (Motoyama et al. 1994), L-glutamate (Motoyama et al. 1993), and L-lysine (Motoyama et al. 2001) have been demonstrated. Despite previous successes, many hurdles remain before industrial applications. In particular, genetic tool development and physiological studies of methylotrophic bacteria are needed for further strain engineering (Schrader et al. 2009). An alternative is to enable methanol assimilation or even bestow methylotrophic growth on strains suitable for industrial processing. In principle, synthetic methylotrophy can be achieved by overexpressing heterologous enzymes for methanol oxidation and engineering a formaldehyde assimilation pathway to produce central metabolites for growth. Methanol oxidation is categorized into three

groups of enzymes based on their terminal electron acceptors: (1) Pyrroloquinoline quinone (PQQ)-dependent methanol dehydrogenases (Mdhs), (2) methanol oxidases, and (3) NAD-dependent Mdhs. NAD-dependent Mdhs are within metal-containing group III alcohol dehydrogenases (Adhs), named Mdh when the enzymes present significant methanol activity, such as *Bacillus methanolicus* Mdhs (De Vries et al. 1992). Group III Adhs are structurally unrelated to group I or II Adhs and are highly diverse (Elleuche and Antranikian 2013). Among the three types of methanol-oxidizing enzymes, NAD-dependent Mdhs are the favorable option for synthetic methylotrophy due to their applicability in both aerobic and anaerobic conditions (Whitaker et al. 2015). Furthermore, electrons derived from methanol oxidation are stored in NADH, which can be used to drive production of target metabolites without sacrificing additional carbons. As such, this type of enzyme was used in a redox balanced methanol condensation cycle (MCC) to achieve conversion of methanol to higher alcohols (Bogorad et al. 2014). In addition, an NAD-dependent Mdh of *B. methanolicus* was introduced in *Escherichia coli* and *Corynebacterium glutamicum* to demonstrate methanol assimilation via the ribulose monophosphate pathway (Müller et al. 2015; Witthoff et al. 2015).

To our knowledge, NAD-dependent Mdhs with relatively high activity have only been reported in the Gram-positive, thermophilic methylotroph, *B. methanolicus* (Arfman et al. 1989; Hektor et al. 2002; Krog et al. 2013), with a few homologs reported from other Gram-positives, both mesophilic and thermophilic bacteria (Sheehan et al. 1988; Ochsner et al. 2014). The existence of NAD-dependent Mdhs in thermophiles is in agreement with the thermodynamic argument that NAD^+-dependent methanol oxidation is favorable at high temperatures (Whitaker et al. 2015). Their sequences have 45–53 % similarity to the NAD-dependent 1,3-propanediol dehydrogenase of *Klebsiella pneumoniae* (Krog et al. 2013). In contrast to the PQQ-dependent Mdhs which exhibit high methanol specificity (Keltjens et al. 2014), NAD-dependent Mdhs have broad substrate specificities, with optimum activity to 1-propanol or *n*-butanol and marginal activity to methanol (Sheehan et al. 1988; Krog et al. 2013).

The methanol activity of Mdhs of *B. methanolicus* can be greatly enhanced by an endogenous activator protein ACT, which contains a conserved motif for hydrolyzing nucleoside diphosphates linked to a moiety X (Nudix) (Arfman et al. 1989, 1991, 1997; Hektor et al. 2002; Kloosterman et al. 2002). This activation effect has been found to be widespread among group III Adhs (Ochsner et al. 2014) and results in both increased K_{cat} and decreased K_m. Notably, this activation is general to all substrates, instead of a specific activation for methanol (Krog et al. 2013; Ochsner et al. 2014). ACT activates Mdh by hydrolytically removing the nicotinamide mononucleotide (NMN) moiety of the Mdh-bound NAD, causing a change in its reaction mechanism from the ping-pong type mechanism to the ternary complex mechanism (Arfman et al. 1997). The ACT-Mdh activation model has been proposed to be a reversible process in which the interaction between ACT and Mdh results in conformational change to position NAD^+ and methanol binding sites closer together, thus enabling direct electron transfer (Kloosterman et al. 2002). However, the detailed mechanism of Mdh activation is still unclear. For the purpose of metabolic engineering, it would be useful to identify an Mdh with high activity under mesophilic or thermophilic conditions without the need for ACT.

In this work, we characterized a putative Mdh encoded by *mdh2* in the genome of a non-methylotrophic bacteria *Cupriavidus necator* N-1. We showed that Mdh2 was an active NAD-dependent Mdh without the need for ACT. Mdh2 is the first group III Adh identified in Gram-negative, mesophilic bacteria that possesses significant methanol activity. Using directed evolution, we further improved the Mdh activity and specificity for methanol.

Material and methods

Reagents

All chemicals were purchased from Sigma-Aldrich or Fisher Scientific unless otherwise specified. KOD Xtreme DNA polymerases were purchased from EMD Biosciences (San Diego, CA, USA). Phusion Hot Start II High-Fidelity DNA polymerases were purchased from Thermo Scientific (Waltham, MA, USA). DpnI enzymes were purchased from New England Biolabs (Ipswich, MA, USA).

Strains and plasmids

The complete plasmids and primers list used in this work is shown in Table 1. *E. coli* XL-1 blue was used as the cloning strain to propagate all plasmids. *C. necator* N-1 strain (ATCC43291) was purchased from ATCC (Manassas, VA, USA) and the genomic DNA was extracted by Qiagen (Valencia, CA, USA) DNeasy Blood & Tissue Kit.

PCR amplification and cloning

The annotated *mdh1* (CNE_2c07940) and *mdh2* (CNE_2c13570) genes from *C. necator* N-1 genome were found from Uniprot protein data base (The Uniprot Consortium 2015). The inserted *mdh1* gene on plasmid pCT23 was amplified from *C. necator* N-1 genomic DNA using primers CT74 and CT75 (Table 1). The inserted *mdh2* gene on plasmid pCT20 was amplified from *C. necator* N-1 genomic DNA using primers CT64 and CT65 (Table 1). The inserted *nudF* gene on plasmid pTW195 was amplified from *E. coli MG1655* (ATCC700926) genomic DNA using primers

Table 1 List of plasmids and primers used in this work

Plasmids	Genotype	Reference
pZE12-luc	AmpR; ColE1 ori; $P_{LlacO-1}$:: *luc(PP)*	Lutz and Bujard (1997)
pIB4	AmpR; ColE1 ori; $P_{LlacO-1}$:: *fbp(EC)-fxpk(BA)*, with lacI	Bogorad et al. (2013)
pCT20	Amp^R; derivative of pIB4 with *mdh2* (*C. necator* N-1)	This study
pCT23	Amp^R; derivative of pIB4 with *mdh1* (*C. necator* N-1)	This study
pCT20_10C12	Amp^R; derivative of pIB4 with *mdh2* (A31V)	This study
pCT20_4D8	Amp^R; derivative of pIB4 with *mdh2* (A169V)	This study
pCT20_15E9	Amp^R; derivative of pIB4 with *mdh2* (A26V, A169V)	This study
pTW212	Amp^R; derivative of pIB4 with *mdh2* (A26V)	This study
pCT20_S1	Amp^R; derivative of pIB4 with *mdh2* (A26V, A31V, A169V)	This Study
pCT20_A169I	Amp^R; derivative of pIB4 with *mdh2* (A169I)	This study
pCT20_A169L	Amp^R; derivative of pIB4 with *mdh2* (A169L)	This study
pCT20_A169M	Amp^R; derivative of pIB4 with *mdh2* (A169M)	This study
pCT20_A169P	Amp^R; derivative of pIB4 with *mdh2* (A169P)	This study
pCT20_A169C	Amp^R; derivative of pIB4 with *mdh2* (A169C)	This study
pQE9-Act(Bm)	Amp^R; derivative of pIB4 with *act* (*B. methanolicus* PB1)	This study
pTW113	Amp^R; derivative of pIB4 with *adhA* (*C. glutamicum* 534)	This study
pTW195	Amp^R; derivative of pIB4 with *nudF* (*E.coli* MG1655)	This study; Ochsner et al. 2014
pMS4	Amp^R; derivative of pIB4 with CNE_BB1p03180 (*C. necator* N-1)	This study
pMS5	Amp^R; derivative of pIB4 with CNE_1c08460 (*C. necator* N-1)	This study
pMS12	Amp^R; derivative of pIB4 with CNE_1c14320 (*C. necator* N-1)	This study
pMS13	Amp^R; derivative of pIB4 with CNE_1c04760 (*C. necator* N-1)	This study
pMS14	Amp^R; derivative of pIB4 with CNE_1c10080 (*C. necator* N-1)	This study
Primer name	Sequence 5′->3′	
T989	TCTAGAGGCATCAAATAAAACGAAA	
T990	TCCCTGAAAATACAGGTTTTCGGAT	
T1151	atccgaaaacctgtattttcagggaATGACCACTGCTGCACCCCA	
T1152	tttcgttttatttgatgcctctagaTTAGAAACGAATCGCCACAC	
T1478	ATCCGAAAACCTGTATTTTCAGGGAATGCTTAAGCCAGACAACCT	
T1479	TTTCGTTTTATTTGATGCCTCTAGATTATGCCCACTCATTTTTTA	
IWB094	TCTAGAGGCATCAAATAAAACGAAAGGC	
IWB141	TCCCTGAAAATACAGGTTTTCGGATCCGTGATGGTGATGGTGATGCGATCC	
IWB445	TCCGAAAACCTGTATTTTCAGGGAATGGGAAAATTATTTGAGGAAAAAACAATTAAAAC	
IWB446	GCCTTTCGTTTTATTTGATGCCTCTAGATCATTTATGTTTGAGAGCCTCTTGAAGCTGC	
CT64	GGATCCGAAAACCTGTATTTTCAGGGAATGACCCACCTGAACATCGCTA	
CT65	GAGCCTTTCGTTTTATTTGATGCCTCTAGATTACATCGCCGCAGCGAAGATTGCC	
CT74	CGGATCCGAAAACCTGTATTTTCAGGGAATGATCCATGCCTACCACAACC	
CT75	CCTTTCGTTTTATTTGATGCCTCTAGACTAGGCAGACACGGCGCCGATAAA	
CT291	CGAGCAATCATGTGAAGATGNNKATCGTCGACTGGCGTTGCAC	
CT292	GTGCAACGCCAGTCGACGATMNNCATCTTCACATGATTGCTCG	
MS14	aaaacctgtattttcagggaGAAGTTTATCAAAAGCACTCACATG	
MS15	ttttatttgatgcctctagaTCAACGATCAGGCAAGACTCTTTCA	
MS16	aaaacctgtattttcagggaCGTCCTGCTTTCGATCCCGAATCCC	
MS17	ttttatttgatgcctctagaTCAGGCCGCCAGCAGGTGGTAAAGA	
MS33	aaaacctgtattttcagggaATGAAATTCTGCTCGAACTGTGGTC	
MS34	ttttatttgatgcctctagaTCAGGGCGTGACCGTGGCCCGGCTG	
MS35	aaaacctgtattttcagggaATGTCCTACAAGATCCCGGAATCCG	
MS36	ttttatttgatgcctctagaTCATGGCTGCGCTCCGTACACCGCC	
MS37	aaaacctgtattttcagggaATGACCGACAAGATCCAACGCGGCA	
MS38	ttttatttgatgcctctagaCTATATGGCGTAATGCGGCAGCGGC	

T1478 and T1479 (Table 1). The inserts encoding the putative Nudix genes were amplified from *C. necator* N-1 genomic DNA to create pMS4 (CNE_BB1p03180, primers MS14 and MS15), pMS5 (CNE_1c08460, primers MS16 and MS17), pMS12 (CNE_1c14320, primers MS33 and MS34), pMS13 (CNE_1c04760, primers MS35 and MS36), and pMS14 (CNE_1c10080, primers MS37 and MS38). The insert *adhA* (Cgl2807) gene of plasmid pTW113 was amplified from *Corynebacterium glutamicum* (ATCC 13032D-5) by T1151 and T1152 (Table 1). The backbones of pTW195, pCT20, pCT23, pTW113, and all pMS plasmids were amplified from a modified plasmid pZE12-luc (Lutz and Bujard 1997), pIB4, of which a lacI repressor was included using primers T989 and T990. For plasmid pQE9-Act(Bm), the insert *act* gene was amplified from *B. methanolicus* PB1 genomic DNA using primers IWB445 and IWB446, whereas vector backbone was amplified from pQE9 acquired from Qiagen using primers IWB094 and IWB141. Polymerase chain reactions (PCRs) were conducted using Phusion Hot Start II High-Fidelity or KOD Xtreme DNA Polymerases, followed with DpnI digestion. The DNA products were purified by Zymo DNA clean & concentrator kit (Zymo Research, Irvine, CA, USA). The purified backbone and insert were assembled in a 10 μL reaction using isothermal DNA assembly method (Gibson et al. 2009) at 50 °C for 20 min. Five microliters of the reaction mixture was transformed in 50 μL Zymo Z-competent XL-1 blue competent cell (Zymo research) and plated on LB agar plates containing the appropriate antibiotic. Positive transformants were verified by colony PCR and Sanger sequencing.

Protein purification and SDS-PAGE

The Mdh1 and Mdh2 were synthesized from plasmids pCT20 (Mdh2) and pCT23 (Mdh1) with N-terminal His-tag in *E. coli* strain XL-1 blue. The XL-1 blue strains were cultured 16–20 h aerobically at 37 °C in Luria-Bertani (LB) media supplemented with appropriate antibiotics. The next day, 1 % of overnight culture was inoculated into LB medium with antibiotics and cultured at 37 °C for 2 to 3 h until OD_{600} was around 0.4–0.8, followed by the addition of 0.1 mM isopropyl-β-D-thiogalactopyranoside (IPTG) induction at room temperature (22–25 °C) for 16 to 20 h. Cells were harvested by centrifugation at 4 °C and either used directly or stored in −80 °C for later protein purification. The purification was conducted with Ni-NTA column using glycylglycine based buffers at room temperature. Protein concentration was measured by Coomassie Plus Assay (Thermo Scientific) at OD_{595}. The purified proteins were analyzed on 12 % Mini-PROTEAN TGX gel (Bio-rad, Hercules, CA, USA) and the gel was stained with SimplyBlue SafeStain (Life Technologies, Carlsbad, CA, USA).

Enzyme assays

Mdh activity assays were carried out in a 200-μL assay mixture containing 100 mM sodium bicarbonate buffer (pH 9.5), 30 μg of Mdh, 5 mM of Mg^{2+}, 3 mM NAD^+, and 800 mM of methanol at 30 °C. For C2-C4 alcohol affinity assays, 10 mM ethanol with 1 μg Mdh, 5 mM 1-propanol 5 with 0.5 μg Mdh, and 100 mM *n*-butanol with 0.5 μg Mdh were used instead. For pH assays, buffers pH 6 (2-(*N*-morpholino)ethanesulfonic acid), pH 7 (potassium phosphate), pH 8.5 (glycylglycine), pH 9.5 (sodium bicarbonate), and pH 10.5 (sodium bicarbonate) were used with the same recipe of Mdh activity assay stated above. For thermal stability assays, the reaction mixture (use sodium bicarbonate pH 9.5) containing everything except the initiating substrate (methanol) was pre-incubated at temperatures ranging from 25 to 60 °C in a Bio-rad PCR machine for 10 min before initiating the assay at 30 °C. For temperature activity profile assays, the reaction mixture (use sodium bicarbonate pH 9.5) containing all the components except the enzyme and methanol was pre-incubated at assay temperature for 5 min before starting the assay. All assays were initiated by adding methanol. One microgram of purified his-tagged ACT or NudF was used to test Mdh activation. It should be noted that NAD^+ needs to be added before mixing with Mdh because significant inhibition will be otherwise observed. The activity was defined by the reduction rate of NAD^+ at OD_{340} using Bio-Tek Eon microplate spectrophotometer. One unit (U) of Mdh activity was defined as the amount of enzyme that converts 1 μmol of substrate into product per minute. The K_m values and V_{max} of Mdh were calculated by Prism 6 (GraphPad Software, La Jolla, CA, USA).

High throughput screening (HTS): Nash reaction-based screening

Cells were grown overnight in LB medium supplemented with 20 mM $MgCl_2$, 0.1 mM IPTG, and appropriate antibiotics. Nash reagent was prepared by dissolving 5 M ammonium acetate and 50 mM acetylacetone in M9 buffer. Before the assay, cell density was determined by OD_{595}. The assay was started by mixing 100 μL of overnight cell culture, 80 μL Nash reagent, and 20 μL 5 M methanol in 96-well plate (#3370, Corning, Corning, NY, USA). After 3 h of incubation in 37 °C shaker (250 rpm), the reaction mixture was centrifuged at 3500× rpm (Allegra X14-R centrifuge, rotor SX4750, Beckman Coulter, Brea, CA, USA) for 10 min. One hundred microliters of supernatant was transferred to a fresh 96-well plate, from which OD_{405} measurement was taken. All the OD measurements were accomplished on Victor 3V plate reader (Perkin Elmer, Waltham, MA, USA). For the quantification of the Nash reaction and cell density, we substituted OD_{595} and OD_{405} for OD_{600} and OD_{412}, respectively.

High throughput screening (HTS): library construction and procedure

The random mutagenesis libraries for HTS were constructed by GeneMorph II EZClone mutagenesis kit (Agilent, Santa Clara, CA, USA) following manufacturer's protocol. In short, 10 ng of parent Mdh DNA was used as the template for primers CT64 and CT65 for error-prone PCR. The error-prone PCR was carried out for 30 thermal cycles and resulted in an average error rate of 2 nt/kb. The error-prone PCR product was gel-purified (Zymoclean gel DNA recovery kit, Zymo Research) and assembled to a backbone based on pCT20. The assembled library was transformed to the *E. coli* strain DH10B (Life Technologies) by electroporation and plated on Bioassay QTrays (Molecular Devices, Sunnyvale, CA, USA) containing 200 mL LB agar (1.5 % *w/vol*) with appropriate antibiotics. From the Bioassay QTrays, single colonies were picked by a QBot colony picker (Molecular Devices) and inoculated into 96-well low profile plates (X6023, Molecular Devices) containing 150 μL of LB supplemented with 15 % (*v/v*) glycerol, 1 % (*w/vol*) glucose, and appropriate antibiotics. As positive control, 96 colonies containing the wild-type Mdh or parent Mdh were picked into a single 96-well plate and processed together with other plates. Similarly, colonies containing *E. coli* transketolase (Tkt) was used as the negative control. The plates were covered with a lid and grown overnight in a 37 °C the incubator. Subsequently, plates were used to re-inoculate a fresh 96-well plate (#3370, Corning) filled with 200 μL LB supplemented with 20 mM $MgCl_2$, 0.1 mM IPTG, and appropriate antibiotics. The new plate was sealed with aluminum sealing film (#6569, Corning) and incubated in 37 °C shaker (250 rpm), while the old plate was kept in −80 °C as stock. After about 16 h of growth, the culture plates were transferred to the BenchCel 4R system with Vprep Velocity11 liquid handler (Agilent) using a 96 LT head. The cells were gently re-suspended and 100 μL of the samples was aliquoted to a fresh 96-well plate (#3370, Corning). Cell density was assessed by OD_{595} at this point. After the measurement, Mdh variants were assessed by the Nash reaction in a 96-well format at 405 nm using the Victor 3V plate reader (Perkin Elmer) as above.

Site-saturation mutagenesis

The site-saturation mutagenesis on Mdh2 A169 site was constructed by Quikchange II site-directed mutagenesis kit (Agilent) with primers CT291 and CT292. The degenerate codons on the primers generate all possible amino acid substitutions. The library was transformed to *E. coli* DH10β strain and single colonies containing all 19 amino acid substitution variants were isolated for further analysis.

Mdh2 sequence analysis

The Mdh2 amino acid sequence was uploaded to SWISS-MODEL web server (http://swissmodel.expasy.org/) (Guex et al. 2009), which performed the structure analysis and generated a 2D plot to present Mdh2 homologs of existing protein structure repository. The Mdh2 and its homologs were aligned using T-coffee (http://www.tcoffee.org/Projects/tcoffee/) (Notredame et al. 2000) and visualized by ESPript 3.0 web server (ESPript - http://espript.ibcp.fr) (Robert and Gouet 2014).

Results

Expression, purification, and characterization of *C. necator* N-1 Mdh2

To determine whether the two putative Mdhs in *C. necator* N-1, encoded by *mdh1* and *mdh2* genes (gene names designated as in UniProt), exhibit catalytic activity towards methanol, these genes were cloned and expressed from the His-tag plasmids pCT20 (Mdh2) and pCT23 (Mdh1) in *E. coli* XL-1, and the Mdh1 and Mdh2 proteins were purified. SDS-PAGE analysis showed both the purified Mdh1 and Mdh2 were detected with molecular masses of approximately 40 kDa, which is close to the predicted sizes 38.8 and 40.7 kDa for Mdh1 and Mdh2, respectively (Supplementary material Fig. S1). To test whether Mdh1 or Mdh2 shows the desired activity, we performed the methanol dehydrogenase activity assay by monitoring $NAD(P)^+$ reduction. Mdh1 methanol-linked oxidation was not observed when using either NAD^+ or $NADP^+$ as the electron acceptor (data not shown). However, Mdh2 showed significant specific activity 0.32 U/mg (Table 2) when NAD^+ was used as the electron acceptor, whereas no methanol oxidation activity was detected when $NADP^+$ was used. The K_m values of Mdh2 for methanol and NAD^+ were 132 and 0.93 mM, respectively. The specific activity and K_m values of Mdh2 at 30 °C without ACT were comparable to the ACT activated *B. methanolicus* Mdhs at 45 °C (Krog et al. 2013). Examination of the catalytic activity of Mdh2 to C1-C4 alcohols showed that Mdh2 exhibits broad substrate specificity, with highest specificity towards 1-propanol and low affinity to methanol, similar to previously reported Mdhs (Table 2) (Krog et al. 2013).

Effects of pH, temperature, and ions on Mdh2

Further characterization was conducted using methanol as a substrate to investigate the effect of pH, temperature, and different metal ions on Mdh2. As shown in Fig. 1a, the Mdh2 was active from pH 6 to 10.5, with its optimum at pH 9.5. The thermal stability assay revealed that Mdh2 enzyme was

Table 2 Substrate specificity to C1–C4 alcohols and kinetic constants of recombinant Mdh2 in vitro

Substrate	K_m (mM)	K_{cat} (s^{-1})	K_{cat}/K_m (M^{-1} s^{-1})	V_{max} (U/mg)	V_{max}[a] (U/mg) (MGA3 Mdh3, 45 °C)
Methanol	132.1 ± 15.4	0.22 ± 0.01	1.6	0.32	0.07
Ethanol	0.77 ± 0.1	11.1 ± 0.3	14,483	16	1.3
Propanol	0.54 ± 0.1	9.6 ± 0.2	17,759	14.2	2.8
n-Butanol	7.2 ± 1	6.5 ± 0.2	906	9.6	2.6
NAD^+	0.93 ± 0.079	0.24 ± 0.005	258	0.36	–
$NADP^+$	N.D.	N.D.	N.D.	N.D.	–

The values shown indicate mean ± standard deviation. Triplicate experiments were performed. Mdh assays to determine K_m for different alcohols were performed using various alcohol concentrations and 3 mM NAD^+ as substrates at 30 °C and pH 9.5. To determine kinetic parameters of NAD^+, 800 mM of methanol was used and the rest of conditions remained unchanged

[a] The V_{max} values of *B. methanolicus* MGA3 Mdh3 were obtained from published data (Krog et al. 2013)

inactivated (Fig. 1b) when incubating for 10 min at temperatures higher than its physiological growth condition (30 °C). In particularly, 13 % of activity remained after pre-incubation at 55 °C (Fig. 1b) and the activity was abolished at 60 °C. To detect the enzyme sensitivity to various metal ions and EDTA, we performed the assay in the presence of these additives. Figure 2 shows that the activity of Mdh2 was activated by the addition of 1 mM Ni^{2+} and was strongly inhibited by 0.1 mM of Cu^{2+} or Zn^{2+}.

Insensitivity of Mdh2 to ACT

Activation of type III Adhs by the activator protein ACT or its homolog Nudix hydrolase is common, and may even be general for all enzymes in this class (Ochsner et al. 2014). The activation results in drastic improvement in V_{max} and K_m. For instance, six Mdhs of *B. methanolicus* PB1 and MGA3 can be strongly activated by ACT (Krog et al. 2013) at their physiological temperature, 45 °C. To test if Mdh2 from *C. necator* N-1 can be activated by ACT, we cloned and purified a his-tagged thermophilic ACT from *B. methanolicus* PB1 and its mesophilic homolog Nudix hydrolase NudF from *E. coli* (Ochsner et al. 2014). The ACT and NudF were used to activate Mdh2 at various temperatures from 25 to 65 °C. Since *B. methanolicus* PB1 ACT is a thermophilic enzyme, the *E. coli* NudF was used to ensure the activator protein was active under mesophilic temperatures. Mdh3 of *B. methanolicus* MGA3, which was previously shown to be activated by ACT (Krog et al. 2013), served as a positive control. Interestingly, Mdh2 was largely insensitive to ACT and NudF between 25 and 40 °C (Fig. 3a). The activity of Mdh2 was mildly increased by ACT or NudF at 55 °C and 60 °C where it reached the optimum specific activity at 55 °C with 70 % improvement. In contrast, Mdh3 was significantly activated when assay temperature was above 42 °C. At its optimum temperature 60 °C, the specific activity improved more than 15-fold to 0.35 U/mg (Fig. 3b).

To verify if Mdh2 is insensitive to the Nudix proteins from *B. methanolicus* and *E. coli*, we first varied the activator concentration by 10-fold (up to 50 μg/mL). No activation effect

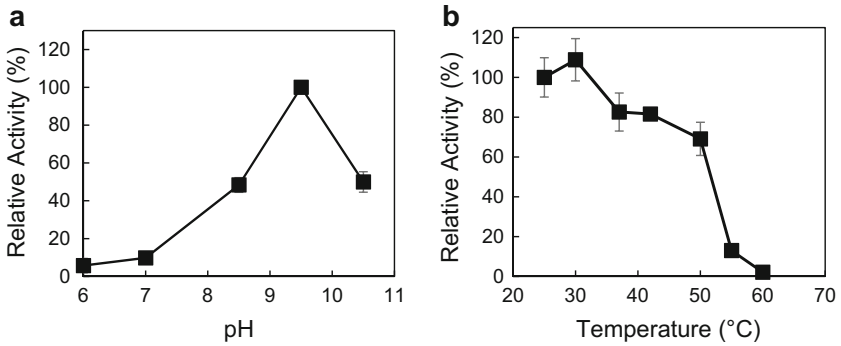

Fig. 1 **a** Effects of pH and **b** thermal stability of *C. necator* N-1 Mdh2. Assays (**a**) were performed using 800 mM methanol and 3 mM NAD^+ as substrates at 30 °C. For assays (**b**), the reaction mixture containing everything except the initiating substrate (methanol) was pre-incubated at temperatures ranging from 25 to 60 °C. Methanol was added to initiate reaction at 30 °C and pH 9.5 to measure remaining activity. The data shown were from triplicate experiments

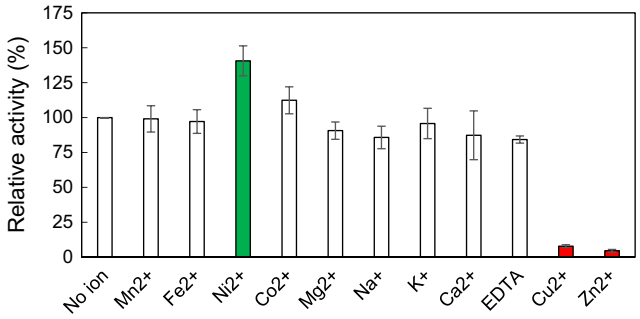

Fig. 2 Effect of ions and chelator to Mdh2. Experiments were performed by incubating enzyme with 1 mM ions (0.1 mM for Cu^{2+} and Zn^{2+}) or EDTA for 3 min, then using 800 mM methanol and 3 mM NAD^+ as substrates at 30 °C and pH 9.5. The highlighted *green color* indicates significant activity increase and *red color* indicates significant activity decrease. The data shown were from triplicate experiments

was observed under the conditions tested (Fig. 4a). In addition, K_m and K_{cat} for methanol and NAD^+ remained unchanged in the presence of *B. methanolicus* ACT or *E. coli* NudF at 30 °C (Table 3). Next, we investigated if Mdh2 can only be activated by unknown native activators in *C. necator*. Mdh2 activity was assayed using purified Mdh2 incubated with *C. necator* N-1 crude extracts at concentrations 50 and 150 μg/mL. However, no activity improvement was observed (Fig. 4b). To investigate this possibility further, we found five Nudix family proteins annotated in the *C. necator* N-1 genome: two hydrolase family proteins (coded by CNE_BB1p03180, CNE_1c08460) and three pyrophosphatases (code by CNE_1c14320, CNE_1c04760, CNE_1c10080). We also used BLAST analysis to identify *B. methanolicus* ACT or *E. coli* NudF homologs in *C. necator* N-1 and obtained no additional possibilities. We individually his-tag cloned and expressed these five putative Nudix genes and purified the proteins using *E. coli* for the activation tests. Consistent with crude extract results, none of these putative Nudix proteins can activate Mdh2 (Fig. 4b).

Development of automatic high throughput screening (HTS) for Mdh evolution

As Mdh2 exhibited significant methanol activity without activator protein in mesophilic conditions, this enzyme represents a promising choice for engineering synthetic methylotrophy. However, the activity and substrate specificity remain low for methanol (Table 2). To solve this problem, we sought to engineer Mdh2 for better performance. An NAD^+ binding site mutation S97G of *B. methanolicus* C1 Mdh had been shown to increase methanol oxidation activity significantly (Hektor et al. 2002). However, the mutation of the corresponding residue (S106G) on Mdh2 did not show methanol oxidation activity (data not shown). Another group modified *B. stearothermophilus* Adh, which has methanol oxidation activity, to become hydrogel forming enzyme by outfitting it with cross-linking domains (Kim et al. 2013). Although the modification remarkably increased the in vitro methanol oxidation activity, the feasibility of applying hydrogel forming enzymes in metabolic engineering needs to be further investigated.

To engineer Mdh, we developed an automatic HTS strategy based on automatic liquid handling, colony picking, incubation, and whole cell assay without lysis. Nash reaction (Nash 1953) allows Mdh assay without cell lysis, which detects formaldehyde produced from methanol oxidation by reacting with acetylacetone and ammonium acetate. The reaction product, diacetyldihydrolutidine, exhibits yellow color (Fig. 5a) and can be quantified by absorbance at 405 nm. Since formaldehyde is able to diffuse through the cell membrane, Nash reaction-based screening does not require cell lysis. This greatly simplified the screening procedure and bypassed the background interference in cell crude extracts.

The scale of the screening was enhanced with utilizing automated colony picker and liquid handler as described in the "Material and methods." After integrating all equipment

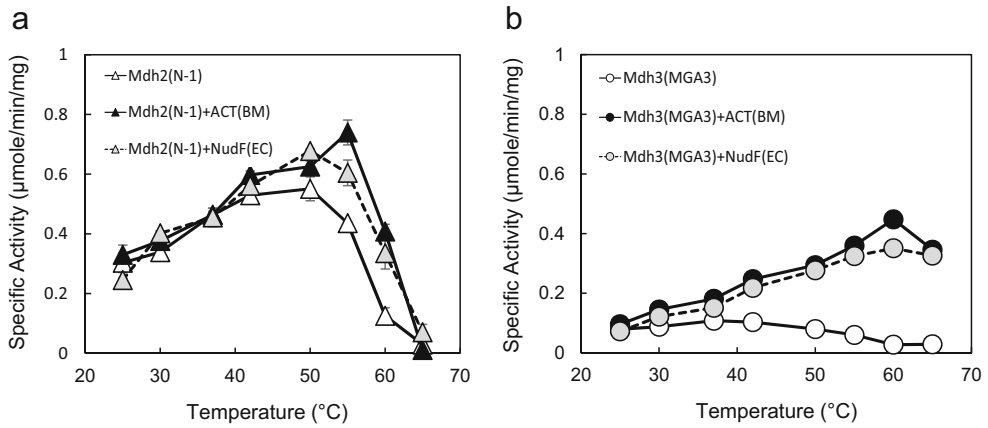

Fig. 3 Effect of activator at different temperatures with **a** Mdh2 of *C. necator* N-1; **b** Mdh3 of *B. methanolicus* MGA3. Assays were performed using 800 mM methanol and 3 mM NAD^+ as substrates at 30 °C and pH 9.5. ACT(BM) indicates the ACT of *B. methanolicus* (thermophilic ACT) and NudF(EC) indicates the ACT homolog NudF of *E. coli* (mesophilic ACT). N-1, *C. necator* N-1. MGA3, *B. methanolicus* MGA3. BM, *B. methanolicus*. EC, *E. coli*. The data shown were from triplicate experiments

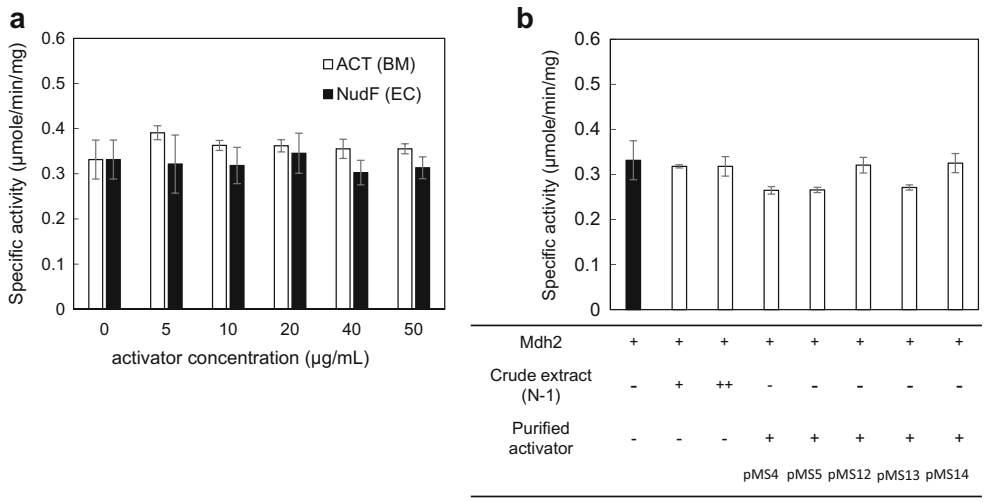

Fig. 4 Mdh2 insensitivity to activation effect. **a** Effect of different activator concentrations to Mdh2 activity. **b** Effect of putative activator proteins of *C. necator* N-1. ACT(BM) indicates the ACT of *B. methanolicus* (thermophilic ACT) and NudF(EC) indicates the ACT homolog NudF of *E. coli* (mesophilic ACT). Mdh2 activity was measured in the presence of crude extract (50 (+) or 150 (++) μg/mL) or 5 μg/mL purified activator using standard Mdh assay at 30 °C and pH 9.5. pMS4 (CNE_BB1p03180 of *C. necator* N-1), pMS5 (CNE_1c08460 *C. necator* N-1), pMS12 (CNE_1c14320 *C. necator* N-1), pMS13 (CNE_1c04760 *C. necator* N-1), pMS14 (CNE_1c10080 *C. necator* N-1). "+" sign indicates addition of protein in the assay. The data shown were from triplicate experiments

into the work flow, the initial design was capable to screen 6000 colonies in a single round using 384-well plates to carry the samples. The readout of Nash reaction was normalized to cell density (OD_{595}). Although the process successfully displayed Mdh activity in colorimetric reading, no improved Mdh was obtained from the first few testing rounds due to high false positive rate. The setback prompted us to inspect the screening accuracy of the initial design. Zhang et al. had developed a standard measure to evaluate and validate the quality of HTS assays (Zhang et al. 1999). The so-called Z′-factor is a statistical characteristic of any given assay with the value between 0 and 1. The Z′-factor was calculated from the positive control and negative control of an assay: a value larger than 0.5 indicates a large separation between the populations of the measured signals and the assay will be considered as high quality. To evaluate our HTS system, strains containing wild-type Mdh2 or Tkt was tested as positive and negative controls, respectively. Three hundred eighty-four single colonies of each control were picked and assayed by Nash reaction. The resulting Z′-factor was 0.23 (Fig. 5b), suggesting the low quality of the initial HTS design.

While revisiting the details of the process, we noticed that the small well dimension of 384-well plates might be constraining mixing during Nash reaction even with shaking. To test the hypothesis that the inaccuracy of the system originated from mixing during Nash reaction, 96-well plates were used to replace 384-well plate in the HTS process. After adjusting the process according to the new plate, the Z′-factor improved to 0.76 (Fig. 5b). This Z′ indicated that the HTS system was suitable for screening for Mdh mutants of high activity and was properly validated. The optimized HTS process is shown in Fig. 5c.

Table 3 Effect of activator proteins on kinetic parameters of recombinant Mdh2 in vitro

Substrate	Activator protein	K_m (mM)	K_{cat} (s^{-1})	K_{cat}/K_m (M^{-1} s^{-1})	V_{max} (U/mg)
Methanol	–	132.1 ± 15.4	0.22 ± 0.01	1.6	0.32
Methanol	*B. methanolicus* ACT	100.7 ± 16.1	0.22 ± 0.01	2.2	0.33
Methanol	*E. coli* NudF	122.1 ± 18.2	0.23 ± 0.01	1.9	0.35
NAD^+	–	0.93 ± 0.079	0.24 ± 0.005	258	0.36
NAD^+	*B. methanolicus* ACT	0.93 ± 0.11	0.20 ± 0.006	215	0.30
NAD^+	*E. coli* NudF	1.3 ± 0.33	0.21 ± 0.02	162	0.31

The values shown indicate mean ± standard deviation. Triplicate experiments were performed. Mdh assays to determine K_m were performed using various methanol concentrations and 3 mM NAD^+ as substrates at 30 °C and pH 9.5. To determine kinetic parameters of NAD^+, 800 mM of methanol was used with various NAD^+ concentrations

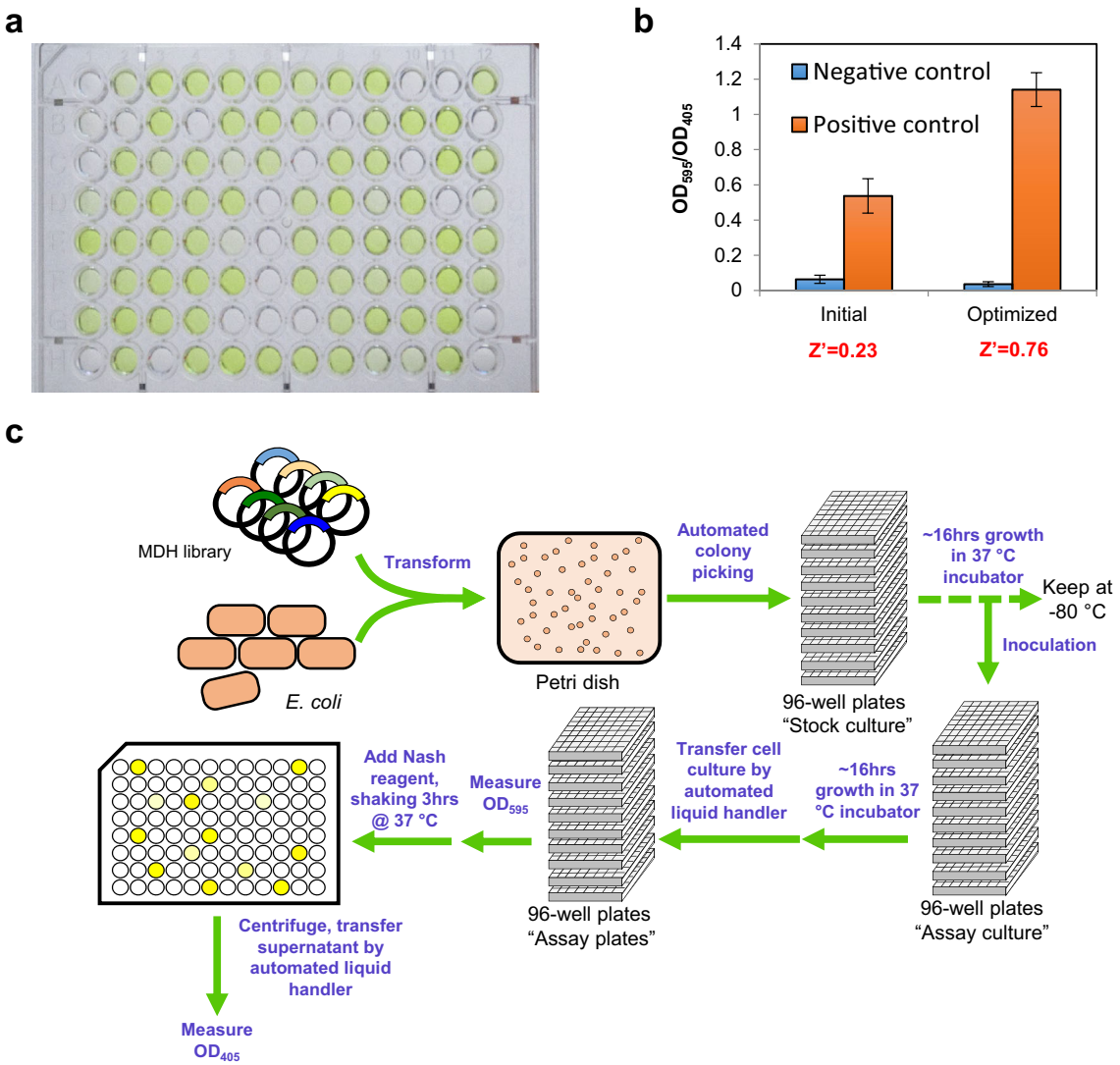

Fig. 5 Development of HTS for Mdh. **a** Utilizing the colorimetric Nash reaction to measure Mdh activity. The *yellow color* indicates reaction product diacetyldihydrolutidine and can be quantified by OD_{405}. **b** Optimization of HTS process by showing improved Z′-factor. Wild-type Mdh2 was used as the positive control and *E. coli* transketolase was used as the negative control. **c** Schematic diagram of Mdh HTS process

Directed evolution of Mdh2

We started the Mdh evolution with error-prone PCR-generated library using the wild-type *mdh2* from *C. necator* N-1 as the template. The first round of screening generated 8 possible positive variants with 50 % or higher activity improvement based on Nash reaction out of 2000 variants screened. These variants were sequenced and tested by NADH-based assay for crude extract activity to eliminate the false positives. Variants CT1-1 and CT1-2 displayed the highest improved activity based on the crude extract assay and were selected for purification and further characterization. Purified variant CT1-2 showed a 5-fold decrease in K_m, while CT1-1 improved marginally in K_m and K_{cat} (Table 4). However, K_{cat} of CT1-2 decreased by almost 50 % compared to the wild-type.

In the second round of screening, CT1-2 was used as the parent to generate another error-prone PCR library. Seven possible positive variants with at least 70 % activity improvement by Nash reaction were obtained from total of 2000 screened. After confirmation by sequencing and crude extract activity assay, only variant CT2-1 was selected for characterization. Variant CT2-1 restored wild-type K_{cat} while maintaining the K_m improvement (Table 4). In addition to the mutation A169V that originated from the previous screen, CT2-1 included another mutation, A26V. To determine the effect of A26V, we introduced this mutation in the wild-type *mdh2* and determined its effect after purification. Interestingly, the mutation A26V alone demolished Mdh activity (Table 4), suggesting a synergistic effect of mutation A26V and A169V in enzyme function.

Table 4 Kinetic parameters of engineered Mdh2 variants to methanol and *n*-butanol, using NADH as cofactor

Mdh2 variant	Library	Mutations	Nash activity	Methanol			*n*-Butanol		
				K_m (mM)	K_{cat} (s^{-1})	K_{cat}/K_m (M^{-1} s^{-1})	K_m (mM)	K_{cat} (s^{-1})	K_{cat}/K_m (M^{-1} s^{-1})
WT	–	–	1.00	132 ± 15.4	0.22 ± 0.01	1.6	7.2 ± 2.1	6.5 ± 0.1	903
CT1-1	Round 1	A31V	1.45	129 ± 11.9	0.25 ± 0.01	1.9	11.3 ± 1.3	7.2 ± 0.2	637
CT1-2	Round 1	A169V	1.47	26.9 ± 2.7	0.13 ± 0.003	4.8	66.5 ± 11.8	3.3 ± .0.1	50
CT2-1	Round 2	A26V, A169V	2.96	30.7 ± 3.6	0.21 ± 0.01	6.8	75.9 ± 1.1	5.0 ± 0.2	66
CT2-2	–	A26V	ND	ND	ND	ND	ND	ND	ND
CT4-1	Recombination	A26V, A31V, A169V	3.46	21.6 ± 1.5	0.20 ± 0.01	9.3	120 ± 17.9	5.7 ± 0.4	48

After these rounds of HTS, a chimeric variant CT4-1 was created by recombining three mutations found so far (A169V, A31V, and A26V). The K_m value of methanol was further lowered to 21.6 mM and K_{cat} remained unchanged (Table 4). Variant CT4-1 represented the best performing variant from the series of engineering with about 6-fold higher K_{cat}/K_m ratio towards methanol compared to the wild-type.

Substrate specificity of the evolved Mdh2

To characterize the kinetic parameters of Mdh variants toward longer chain alcohols, *n*-butanol was chosen as an example to measure K_m and K_{cat}. Results indicates that K_m values for *n*-butanol were increased by 10-fold or higher (Table 4) for variants CT1-2, CT2-1, and CT4-1. The increased K_m towards *n*-butanol was concomitant with the decrease of K_m towards methanol. The best variant, CT4-1, displayed the most significant 19-fold decrease in K_{cat}/K_m towards *n*-butanol among all variants. To further investigate substrate preferences on other higher alcohols, the specific activities towards ethanol and propanol were measured at the concentrations that saturate wild-type Mdh2 activity (Fig. 6a). Consistent with the *n*-butanol data, variants CT1-2, CT2-1, and CT4-1 showed 5- to 10-fold lowered specific activity towards ethanol and 6- to 8-fold lowered for propanol. As summarized in Fig. 6b, CT4-1 significantly improved its methanol over C2 to C4 alcohol activity ratio compares to wild-type.

Sequence analysis

The Mdh2 amino acid sequence was uploaded to SWISS-MODEL server (Guex et al. 2009) to predict a hypothetical model based on structural information in the database. The server returned a plot of sequence similarity as shown in Fig. 7a. The most structurally similar enzymes were *K. pneumoniae* 1,3-propanediol dehydrogenase (1,3-PDH) and *Zymomonas mobilis ZM4* alcohol dehydrogenase 2 (Adh2) with 55 and 54 % sequence identities, respectively. Both enzymes were categorized as group III metal-dependent dehydrogenases and contained Fe^{2+} in their catalytic centers (Marçal et al. 2009; Moon et al. 2011). Notably, Mdh2 also has 55 % sequence identity to *B. methanolicus* MGA3 Mdh,

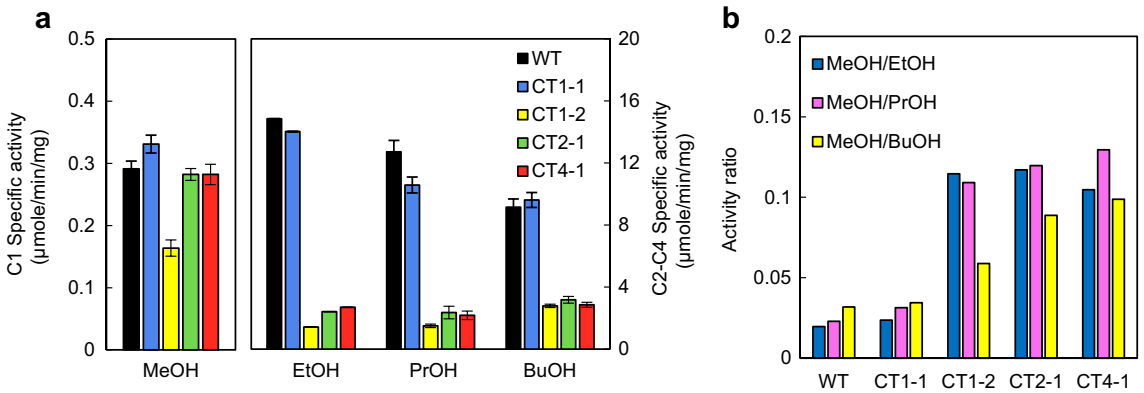

Fig. 6 **a** C1 to C4 alcohol specificity of Mdh2 and its engineered variants. Alcohol concentrations used in the activity assays: MeOH, 800 mM; EtOH, 10 mM; PrOH, 5 mM; BuOH, 100 mM. **b** Activity ratio of methanol over longer chain alcohols (C2 to C4). WT, Mdh2; CT1-1, A31V; CT1-2, A169V; CT2-1, A26V, A169V; CT4-1, A26V, A31V, A169V. NAD^+ 3 mM and alcohol concentrations saturate activity of wild-type Mdh2 were chosen for assay conditions and the assays were performed at 30 °C and pH 9.5. The data shown were from triplicate experiments

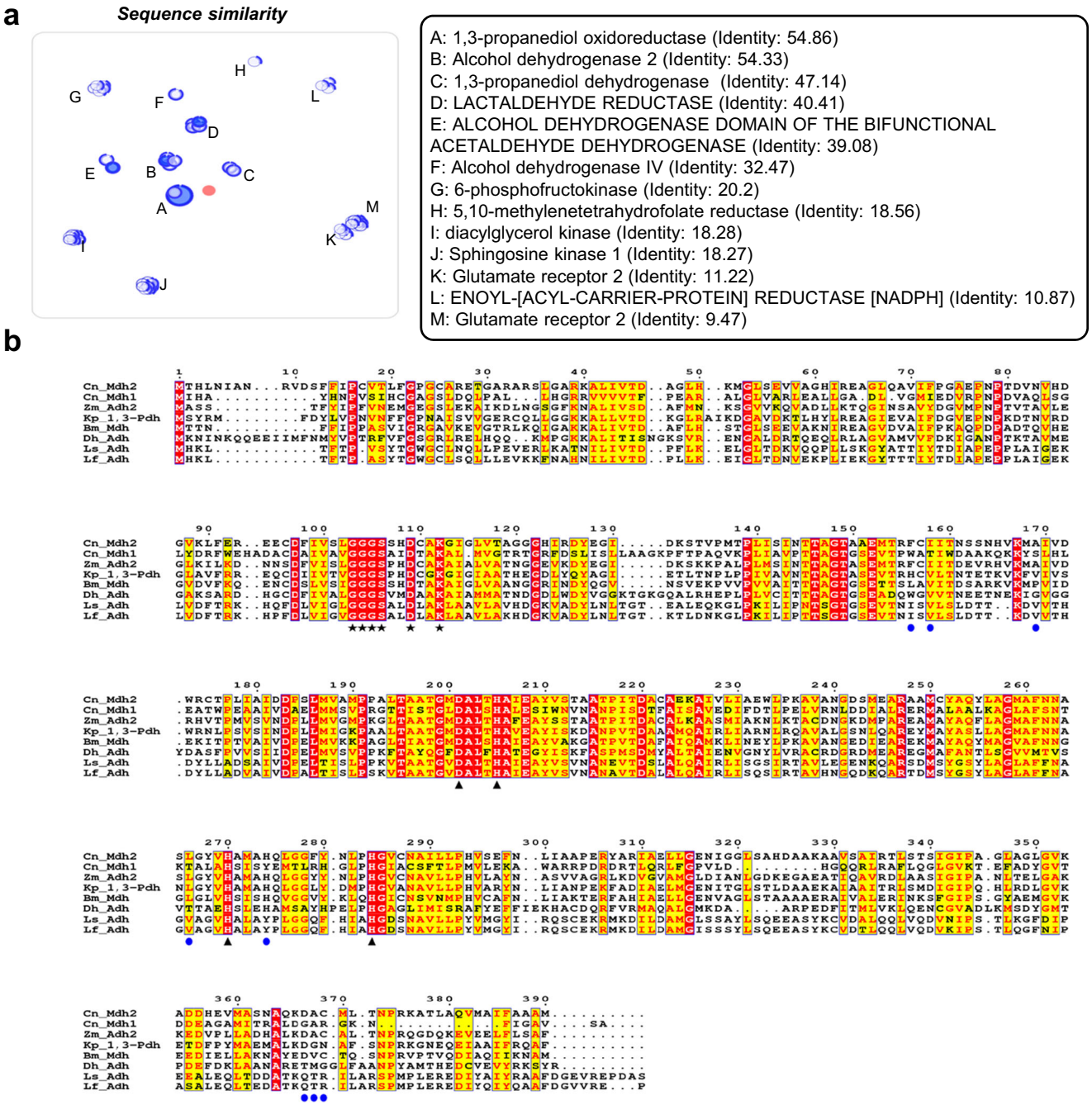

Fig. 7 Sequence information of *C. necator* N-1 Mdh2. **a** Sequence similarity predicted by SWISS-MODEL protein structure homology modeling. Mdh2 was shown as *red circle* in the middle, each template enzyme was shown as a *blue circle* which clusters with a group of similar enzymes. The distance between two template enzymes is proportional to the sequence identity. **b** Sequence alignment of group III alcohol dehydrogenases/methanol dehydrogenase and recently identified methanol-oxidizing Adhs. Cn, *C. necator* N-1; Zm, *Z. mobilis* ZM4; Kp, *K. pneumoniae*; Bm, *B. methanolicus* MGA3; Ls, *L. sphaericus* C3-41; Lf, *L. fusiformis* ZC1; Dh, *D. hafniense* Y51. Amino acid residues that are highly conserved are enclosed by *blue boxed* and *highlighted in yellow*. Identical residues are *highlighted in red background*. The NAD^+ binding motif and metal coordination domain are annotated by *black stars and triangles*, respectively. Predicted residues of substrate binding based on Zm_Adh2 are indicated by *blue circles*

which also belongs to group III dehydrogenases. The structure of group III dehydrogenases can be divided into N-terminal domain and C-terminal domains, which are responsible for $NAD(P)^+$ and metal ion binding, respectively. The metal ion coordination motif composed mainly of two to three histidine residues (Carpenter et al. 1998; Ruzheinikov et al. 2001; Montella et al. 2005; Marçal et al. 2009; Moon et al. 2011). In *K. pneumoniae* 1,3-PDH and *Z. mobilis ZM4* Adh2, there

were three histidine and one aspartic acid. These four amino acid residues were conserved in all of the enzymes aligned (Fig. 7b), corresponding to D201, H205, H270, and H284 in Mdh2. On the other hand, the NAD-binding motif ($GGGSX_2DX_2K$) was also observed in the alignment (Fig. 7b) (Wierenga et al. 1986). Taken together, the similarity of both amino acid sequences and functional domains indicated that Mdh2 belongs to group III metal-dependent dehydrogenases. Previously, NAD-dependent Adhs from *Lysinibacillus sphaericus* C3-41, *Lysinibacillus fusiformis* ZC1, and *Desulfitobacterium hafniense* Y51 were identified with methanol oxidation activity (Müller et al. 2015). Alignment with other Mdhs revealed that these methanol-oxidizing dehydrogenases shared the common NAD-binding domain and metal coordination motif (Fig. 7b).

Among the mutations acquired during Mdh2 evolution, A169V contributed significantly to the K_m decrease in methanol. The same mutation also greatly reduced the activity toward C2-C4 aliphatic alcohols. *Z. mobilis* Adh2 is one of the most structurally similar enzymes to Mdh2 and its binding pocket had been predicted (Moon et al. 2011). Residue A169 is one of the predicted binding pocket residues, which were conserved between *Z. mobilis* Adh2 and Mdh2 (Fig. 7b). Therefore, we hypothesized that the change of alanine to bulkier valine reduces the binding space and subsequently hinders larger substrate binding. To test this hypothesis and explore the best possible amino acid substitution at A169, a site-saturation mutagenesis library of A169 was constructed. The specific activities of all 19 variants were measured by Nash reaction (Supplementary material Fig. S2), six best variants were selected for characterization. Although three of the variants with bulkier side chains (A169V, A169I, A169C) showed lower K_m for methanol, the others displayed the opposite (Table 5). Presumably, the K_m improvement is determined by both size and functional groups in the amino acid side chain. In agreement with this note, extremely large (F, W, Y) or small (G) amino acids at A169 showed no activity (Supplementary material Fig. S2). Interestingly, A169P displayed higher K_{cat} as well as K_m (Table 5). Although protein structure characterization would be required to define the role of residue A169, the results here showed that A169 is crucial to Mdh2 activity and substrate preference.

Table 5 Effect of A169 replacement to Mdh2 methanol specificity

Mdh2 variant	K_m (mM)	K_{cat} (s^{-1})	K_{cat}/K_m (M^{-1} s^{-1})	K_{cat}/K_m Fold change
WT	132 ± 15.4	0.22 ± 0.01	1.6	–
A169V	26.9 ± 2.65	0.13 ± 0.003	4.8	3
A169I	68.9 ± 9.0	0.064 ± 0.002	0.93	0.58
A169L	201 ± 31.5	0.093 ± 0.004	0.46	0.29
A169M	203 ± 25.5	0.073 ± 0.002	0.36	0.23
A169P	303 ± 34.9	0.41 ± 0.014	1.4	0.88
A169C	46.0 ± 3.34	0.16 ± 0.003	3.5	2.2

Discussion

NAD-dependent methanol oxidation presents a principal step in utilizing methanol as a substrate for microbial production of chemicals. Mdhs reported heretofore from *B. methanolicus* (Krog et al. 2013) and a few additional homologs (Ochsner et al. 2014) require ACT and thermophilic conditions at 50 °C to activate methanol oxidation activity. A recent report (Müller et al. 2015) also presents challenges in activation of recombinant *B. methanolicus* Mdh in *E. coli* under mesophillic conditions. Despite previously reported as being NAD-dependent, type I Adhs from human liver, horse liver, yeast, and *C. glutamicum*, and *Bacillus stearothermophilus* which exhibited moderate enzymatic activity toward methanol without the requirement for activation (Mani et al. 1970; Sheehan et al. 1988; Kotrbova-Kozak et al. 2007), successful attempts of methanol assimilation were only reported using Mdhs from *B. methanolicus* (Müller et al. 2015; Witthoff et al. 2015). Unfortunately, unlike PQQ-dependent Mdhs, NAD-dependent Mdhs exhibit broad substrate specificity and only show moderate activity towards methanol. In this work, we characterized and engineered a NAD-dependent methanol dehydrogenase, Mdh2, from a non-methylotrophic bacteria *C. necator* N-1 in the recombinant host *E. coli*. Mdh2 represents the first identified group III Adh in Gram-negative, mesophilic organism to exhibit significant activity towards methanol. Wild-type Mdh2 exhibits methanol oxidation activity 0.32 U/mg and K_m value 132 mM at 30 °C, and is insensitive to activation under mesophilic temperatures. After protein evolution using HTS, the best variant CT4-1 retained methanol oxidation activity with remarkable K_m values 21.6 and 120 mM for methanol and *n*-butanol, respectively.

It should be noted that during HTS of Mdh2, a high methanol concentration (500 mM) was used that presumably favored variants with higher K_{cat}. Interestingly, the results showed that the HTS process was capable of identifying variants with improvement in either K_m (CT1-2 in round 1

Table 6 Comparison of methanol activity on reported mesophilic alcohol dehydrogenase from *Corynebacterium glutamicum*

Mdh/Adh	K_m (mM)	V_{max} (U/mg)	K_{cat} (s^{-1})	K_{cat}/K_m (M^{-1} s^{-1})
Mdh2 (*C. necator* N-1)	132 ± 15.4	0.32	0.22 ± 0.01	1.6
CT4-1 (*C. necator* N-1)	21.6 ± 1.5	0.29	0.20 ± 0.01	9.3
AdhA (*C. glutamicum*)	97 ± 9.8	0.29	0.20 ± 0.01	2.1

showed lower K_m than wild-type, Table 4) or K_{cat} (CT2-1 in round 2 showed higher K_{cat} than CT1-2, Table 4). Although the methanol concentration (500 mM) used in the screening was higher than the K_m of Mdh2, the intracellular methanol concentration might be much lower because of diffusion limitation. Since the cells were not lysed in the Nash assay used in HTS, we have shown that the activity was not saturated even at 500 mM (data not shown), suggesting a possible diffusion limitation into the cell. Under non-saturating methanol concentrations, methanol oxidation rate will be a function of both K_{cat} and K_m. Therefore, improvement in either K_{cat} or K_m could be identified. The best variant CT4-1 has three mutations (A26V, A31V, A169V). It is intriguing that A26V or A31V individually showed no or even a negative effect on K_m or K_{cat}, while together with mutation A169V they significantly improved K_m. Since the crystal structure of Mdh2 has not been solved, it remains unclear how mutations A26V or A31V alter the function of Mdh2. Alignment of Mdh2 with other type III NAD-dependent Adhs (Fig. 7b) also provides very limited insight about the function of A26 and A31 since they are not conserved among the Adhs. Structural studies about Mdh2 will be required to uncover the functions of A26 and A31.

To our knowledge, CT4-1 is the best NAD-dependent, activator-independent Mdh with respect to methanol specificity. It was previously reported that AdhA from *Corynebacterium glutamicum* R exhibits appealing K_m and V_{max} values towards methanol (Kotrbova-Kozak et al. 2007). We cloned this enzyme with a his tag, expressed and purified the protein from *E. coli*. In our hands, the K_m (97 mM) and V_{max} (0.29 U/mg) (Table 6) are significantly different from the reported values (K_m = 3 mM, V_{max} = 0.7 U/mg) (Kotrbova-Kozak et al. 2007) and comparable to the wild-type Mdh2. The difference could possibly be attributed to difference in assay conditions (NAD^+ concentration, buffer, additional metal ions) or unknown reasons. Regardless, under the same enzyme assay condition, CT4-1 has 4.4-fold higher catalytic efficiency than AdhA, mainly owing to the K_m difference. As such, it is suitable for metabolic engineering of organisms for in vivo or in vitro applications. A previous study (Ochsner et al. 2014) suggested that group III Adh activation by ACT homolog Nudix hydrolases represents a common mechanism. However, Mdh2 does not require activation.

Structural analysis and sequence alignment confirmed that Mdh2 belongs to group III Adh, by the high structural similarities to the 1,3-PDH of *K. pneumoniae* and Adh2 of *Z. mobilis* ZM4, in addition to a putative NAD^+ binding motif and metal binding resides. Notably, the two most similar enzymes, *Z. mobilis* Adh2 and *K. pneumoniae* 1,3-PDH, do not have methanol oxidation activity. Similarly, *C. necator* N-1 cannot grow on methanol as a carbon source (data not shown), suggesting that the methanol oxidation may be a gratuitous activity in Mdh2.

Discovery of *C. necator* N-1 Mdh2 opens up the possibility of searching for useful NAD-dependent Mdhs for synthetic methylotrophy from Gram-negative, mesophilic organisms. General perception of Mdhs in Gram-negative, mesophilic methyltrophs are mostly PQQ-dependent enzymes localized in periplasm. In contrast, NAD-dependent Mdhs are localized in bacterial cytoplasm (Keltjens et al. 2014). Despite the fact that *C. necator* N-1 possesses an active Mdh, this organism cannot utilize methanol as a carbon source. It remains unclear the physiological role of *mdh2* in *C. necator* N-1. A possible explanation can be found in recent study on a non-methylotrophic, Gram-positive bacteria *C. glutamicum* which possesses a AdhA for methanol oxidation to CO_2, where methanol served as an auxiliary carbon source for energy generation, of which four essential enzymes alcohol dehydrogenase, acetaldehyde dehydrogenase, mycothiol-dependent formaldehyde dehydrogenase, and formate dehydrogenase are involved (Witthoff et al. 2013). More detailed characterizations on physiological growth conditions and genome analysis for *C. necator* N-1 are necessary to unveil the role of *mdh2*.

Acknowledgments We are grateful to members of Liao laboratory Matthew C. Siracusa, Saro Avedikian, Tuan Trinh, and Jessica Han Pham for experiment assistance.

Compliance with ethical standards This article does not contain any studies with human participants or animals performed by any of the authors.

Funding This work is supported by the Reducing Emissions using Methanotrophic Organisms for Transportation Energy (REMOTE) program of the Advanced Research Projects Agency-Energy (Award: DE-AR0000430). This material is based upon research performed in a renovated collaboratory by the National Science Foundation under Grant No. 0963183, which is an award funded under the American Recovery and Reinvestment Act of 2009 (ARRA).

Conflict of interest All the authors declare that he/she has no conflict of interest.

References

Arfman N, Watling EM, Clement W, van Oosterwijk RJ, de Vries GE, Harder W, Attwood MM, Dijkhuizen L (1989) Methanol metabolism in thermotolerant methylotrophic *Bacillus* strains involving a novel catabolic NAD-dependent methanol dehydrogenase as a key enzyme. Arch Microbiol 152(3):280–288. doi:10.1007/BF00409664

Arfman N, Van Beeumen J, De Vries GE, Harder W, Dijkhuizen L (1991) Purification and characterization of an activator protein for methanol dehydrogenase from thermotolerant *Bacillus* spp. J Biol Chem 266(6):3955–3960

Arfman N, Hektor HJ, Bystrykh LV, Govorukhina NI, Dijkhuizen L, Frank J (1997) Properties of an NAD(H)-containing methanol dehydrogenase and its activator protein from *Bacillus*

methanolicus. Eur J Biochem 244(2):426–433. doi:10.1111/j.1432-1033.1997.00426.x

Bogorad IW, Lin T-S, Liao JC (2013) Synthetic non-oxidative glycolysis enables complete carbon conservation. Nature 502(7374):693–7. doi:10.1038/nature12575

Bogorad IW, Chen C-T, Theisen MK, Wu T-Y, Schlenz AR, Lam AT, Liao JC (2014) Building carbon-carbon bonds using a biocatalytic methanol condensation cycle. Proc Natl Acad Sci U S A 111(45):15928–15933. doi:10.1073/pnas.1413470111

Carpenter EP, Hawkins AR, Frost JW, Brown KA (1998) Structure of dehydroquinate synthase reveals an active site capable of multistep catalysis. Nature 394(6690):299–302. doi:10.1038/28431

De Vries GE, Arfman N, Terpstra P, Dijkhuizen L (1992) Cloning, expression, and sequence analysis of the *Bacillus methanolicus* C1 methanol dehydrogenase gene. J Bacteriol 174(16):5346–5353

Elleuche S, Antranikian G (2013) Bacterial group III alcohol dehydrogenases—function, evolution and biotechnological applications. OA Alcohol 1(1):1–6. doi:10.13172/2053-0285-1-1-489

Gibson DG, Young L, Chuang R-Y, Venter JC, Hutchison CA III, Smith HO (2009) Enzymatic assembly of DNA molecules up to several hundred kilobases. Nat Methods 6(5):343–345. doi:10.1038/nmeth.1318

Guex N, Peitsch MC, Schwede T (2009) Automated comparative protein structure modeling with SWISS-MODEL and Swiss-PdbViewer: a historical perspective. Electrophoresis 30(S1):S162–S173. doi:10.1002/elps.200900140

Hagishita T, Yoshida T, Izumi Y, Mitsunaga T (1996) Efficient L-serine production from methanol and glycine by resting cells of *Methylobacterium* sp. strain MN43. Biosci Biotechnol Biochem 60(10):1604–1607. doi:10.1271/bbb.60.1604

Hektor HJ, Kloosterman H, Dijkhuizen L (2002) Identification of a magnesium-dependent NAD(P)(H)-binding domain in the nicotinoprotein methanol dehydrogenase from *Bacillus methanolicus*. J Biol Chem 277(49):46966–46973. doi:10.1074/jbc.M207547200

Keltjens JT, Pol A, Reimann J, Op den Camp HJM (2014) PQQ-dependent methanol dehydrogenases: rare-earth elements make a difference. Appl Microbiol Biotechnol 98(14):6163–6183. doi:10.1007/s00253-014-5766-8

Kim YH, Campbell E, Yu J, Minteer SD, Banta S (2013) Complete oxidation of methanol in biobattery devices using a hydrogel created from three modified dehydrogenases. Angew Chem Int Ed 52(5):1437–1440. doi:10.1002/anie.201207423

Kloosterman H, Vrijbloed JW, Dijkhuizen L (2002) Molecular, biochemical, and functional characterization of a Nudix hydrolase protein that stimulates the activity of a nicotinoprotein alcohol dehydrogenase. J Biol Chem 277(38):34785–34792. doi:10.1074/jbc.M205617200

Kotrbova-Kozak A, Kotrba P, Inui M, Sajdok J, Yukawa H (2007) Transcriptionally regulated *adhA* gene encodes alcohol dehydrogenase required for ethanol and n-propanol utilization in *Corynebacterium glutamicum* R. Appl Microbiol Biotechnol 76(6):1347–1356. doi:10.1007/s00253-007-1094-6

Krog A, Heggeset TMB, Müller JEN, Kupper CE, Schneider O, Vorholt JA, Ellingsen TE, Brautaset T (2013) Methylotrophic *Bacillus methanolicus* encodes two chromosomal and one plasmid born NAD+ dependent methanol dehydrogenase paralogs with different catalytic and biochemical properties. PLoS One 8(3):e59188. doi:10.1371/journal.pone.0059188

Lutz R, Bujard H (1997) Independent and tight regulation of transcriptional units in *Escherichia coli* via the LacR/O, the TetR/O and AraC/I1-I2 regulatory elements. Nucleic Acids Res 25(6):1203–1210. doi:10.1093/nar/25.6.1203

Mani J-C, Pietruszko R, Theorell H (1970) Methanol activity of alcohol dehydrogenases from human liver, horse liver, and yeast. Arch Biochem Biophys 140(1):52–59. doi:10.1016/0003-9861(70)90009-3

Marçal D, Rêgo AT, Carrondo MA, Enguita FJ (2009) 1,3-Propanediol dehydrogenase from *Klebsiella pneumoniae*: decameric quaternary structure and possible subunit cooperativity. J Bacteriol 191(4):1143–1151. doi:10.1128/JB.01077-08

Montella C, Bellsolell L, Pérez-Luque R, Badía J, Baldoma L, Coll M, Aguilar J (2005) Crystal structure of an iron-dependent group III dehydrogenase that interconverts L-lactaldehyde and L-1,2-propanediol in *Escherichia coli*. J Bacteriol 187(14):4957–4966. doi:10.1128/JB.187.14.4957

Moon J-H, Lee H-J, Park S-Y, Song J-M, Park M-Y, Park H-M, Sun J, Park J-H, Kim BY, Kim J-S (2011) Structures of iron-dependent alcohol dehydrogenase 2 from *Zymomonas mobilis* ZM4 with and without NAD+ cofactor. J Mol Biol 407(3):413–424. doi:10.1016/j.jmb.2011.01.045

Motoyama H, Anazawa H, Katsumata R, Araki K, Teshiba S (1993) Amino acid production from methanol by *Methylobacillus glycogenes* mutants: isolation of L-glutamic acid hyper-producing mutants from *M. glycogenes* strains, and derivation of L-threonine and L-lysine-producing mutants from them. Biosci Biotechnol Biochem 57(1):82–87. doi:10.1271/bbb.57.82

Motoyama H, Yano H, Ishino S, Anazawa H, Teshiba S (1994) Effects of the amplification of the genes coding for the L-threonine biosynthetic enzymes on the L-threonine production from methanol by a gram-negative obligate methylotroph, *Methylobacillus glycogenes*. Appl Microbiol Biotechnol 42(1):67–72. doi:10.1007/s002530050218

Motoyama H, Yano H, Terasaki Y, Anazawa H (2001) Overproduction of L-lysine from methanol by *Methylobacillus glycogenes* derivatives carrying a plasmid with a mutated *dapA* Gene. Appl Environ Microbiol 67(7):3064–3070. doi:10.1128/AEM.67.7.3064-3070.2001

Müller JEN, Meyer F, Litsanov B, Kiefer P, Potthoff E, Heux S, Quax WJ, Wendisch VF, Brautaset T, Portais J-C, Vorholt JA (2015) Engineering *Escherichia coli* for methanol conversion. Metab Eng 28:190–201. doi:10.1016/j.ymben.2014.12.008

Nash T (1953) The colorimetric estimation of formaldehyde by means of the Hantzsch reaction. Biochem J 55(3):416–421

Notredame C, Higgins DG, Heringa J (2000) T-Coffee: a novel method for fast and accurate multiple sequence alignment. J Mol Biol 302(1):205–217. doi:10.1006/jmbi.2000.4042

Ochsner AM, Müller JEN, Mora CA, Vorholt JA (2014) *In vitro* activation of NAD-dependent alcohol dehydrogenases by Nudix hydrolases is more widespread than assumed. FEBS Lett 588(17):2993–2999. doi:10.1016/j.febslet.2014.06.008

Robert X, Gouet P (2014) Deciphering key features in protein structures with the new ENDscript server. Nucleic Acids Res 42(W1):W320–W324. doi:10.1093/nar/gku316

Ruzheinikov SN, Burke J, Sedelnikova S, Baker PJ, Taylor R, Bullough PA, Muir NM, Gore MG, Rice DW (2001) Glycerol dehydrogenase: structure, specificity, and mechanism of a family III polyol dehydrogenase. Structure 9(9):789–802. doi:10.1016/S0969-2126(01)00645-1

Schrader J, Schilling M, Holtmann D, Sell D, Filho MV, Marx A, Vorholt JA (2009) Methanol-based industrial biotechnology: current status and future perspectives of methylotrophic bacteria. Trends Biotechnol 27(2):107–115. doi:10.1016/j.tibtech.2008.10.009

Sheehan MC, Bailey CJ, Dowds BCA, McConnell DJ (1988) A new alcohol dehydrogenase, reactive towards methanol, from *Bacillus stearothermophilus*. Biochem J 252(3):661–666

The Uniprot Consortium (2015) UniProt: a hub for protein information. Nucleic Acids Res 43(D):D204–D212. doi:10.1093/nar/gku989

Whitaker WB, Sandoval NR, Bennett RK, Fast AG, Papoutsakis ET (2015) Synthetic methylotrophy: engineering the production of

biofuels and chemicals based on the biology of aerobic methanol utilization. Curr Opin Biotechnol 33:165–175. doi:10.1016/j.copbio.2015.01.007

Wierenga RK, Terpstra P, Hol WGJ (1986) Prediction of the occurrence of the ADP-binding beta alpha beta-fold in proteins, using an amino acid sequence fingerprint. J Mol Biol 187(1):101–107. doi:10.1016/0022-2836(86)90409-2

Witthoff S, Mühlroth A, Marienhagen J, Bott M (2013) C_1 metabolism in *Corynebacterium glutamicum*: an endogenous pathway for oxidation of methanol to carbon dioxide. Appl Environ Microbiol 79(22):6974–6983. doi:10.1128/AEM.02705-13

Witthoff S, Schmitz K, Niedenführ S, Nöh K, Noack S, Bott M, Marienhagen J (2015) Metabolic engineering of *Corynebacterium glutamicum* for methanol metabolism. Appl Environ Microbiol 81(6):2215–2225. doi:10.1128/AEM.03110-14

Zhang J-H, Chung TDY, Oldenburg KR (1999) A simple statistical parameter for use in evaluation and validation of high throughput screening assays. J Biomol Screen 4(2):67–73